A Model of the Proton

R WAYTE

29 Audley Way, Ascot, Berkshire SL5 8EE, England, UK

email: rwayte@googlemail.com

Abstract. A geometrical/mechanical model of the proton is developed which satisfies general empirical features. A Yukawa / Paris-type potential due to a mesonic field is incorporated into Einstein's equations of general relativity to predict a hadronic force constant, stronger than the fine structure constant by $(137/\sqrt{3})$ times Proton mass is expressed in terms of muonic mass building-blocks. Analysis of the magnetic moment allows substructure modelling, incorporating 2 grades of triplets. Creation of these component parts is described in terms of action-integrals. The gluon field energy holding the triplets together is related to total energy. Uniqueness of electromagnetic charge is attributed to a governing action principle. Finally, a neutron model has been proposed, consisting of a proton core orbited by a heavy-electron.

1.   Introduction

Proton design is much more complicated than the electron model (Wayte, Paper 1) or muon model (Wayte, Paper 2). Although proton charge is exactly equal and opposite to the electronic charge, the proton magnetic moment is nearly 3 times the expected value. In addition, the proton has a strong but short-range hadronic/nuclear force field which does not interact with leptons or electric fields. During high-energy collisions, the proton appears to consist of 3 smaller particles, but the amount of spin held by these individuals is

still debatable. Established QCD theory has offered explanations for most aspects of proton behaviour; see textbooks such as Perkins (2000), Martin & Shaw (1997), Fraunfelder & Henley (1991). However, experiments with spin-directed protons severely strain this theory (Krisch, 1992). Some experiments on proton electric/magnetic form factors indicate a quark-like core plus mesonic cloud field, (Iachello, 2004). Other experiments on electron-nucleon scattering, performed to determine radii of proton and neutrons, have been reviewed by Sick (2005).

In this paper, the proton model is based entirely on our previous electron and muon models, to make them all compatible, including some common physical structures. No dependence upon QCD theory has been necessary to explain the mechanics of a proton itself. In Section (2) the hadronic potential is attributed to a pionic field in agreement with Yukawa and the Paris group. In Section (3), Einstein's equations of general relativity are employed to develop a variation of the Yukawa field and predict a hadronic force constant of $\alpha(137/\sqrt{3})$; i.e. 79 times stronger than the fine structure constant. Total energy of this field is shown to be equal to half the proton mass energy. In Section (4), hard core repulsion is attributed to rapid rotation of the proton core, which modulates the field in the very short range only, making it repulsive. In Section (5), proton magnetic moment is fully analysed in terms of a spin-loop and various descending substructures. A model of 2 grades of triplets is proposed.   In Section (6) proton mass is expressed in terms of muon mass, with due allowance for binding energy. Section (7) covers the creation of the sub-structures in terms of spiralling action integrals. The proton core is found to be constructed like a quintuply-wound filament, through which the charge flows perpetually. This is made of fundamental energy/matter, which is localised in the helical windings and constitutes the proton mass. In Section (8), the gluon field which holds component structures together is discussed in terms of its energy. In Section (9) the uniqueness of electromagnetic charge is investigated with regard to its action. Finally in Section (10) a neutron model is proposed consisting of a proton orbited by a heavy-electron.

Thus, the proton features are all *tangible* and revealed as electromagnetic charge, hadronic force-field, hard-core repulsion, internal confining gluon field, mass relative to leptons, spin angular momentum $\frac{1}{2}\hbar$, magnetic moment and substructure particles. Essential properties are the conservation of energy and momentum at all times, and overall compatibility with relativity theory. All fundamental physical constants and

particle properties have been taken from the latest measured values given in http://physics.nist.gov/constants and http://pdg.lbl.gov.

Postulations of negative energy, extra dimensions, point quarks/particles, Higgs bosons, renormalisation and non-conservation of energy at any instant (implied or actual), have not been necessary in this physical theory.

2.   The hadronic potential

The Klein-Gordon wave equation is usually taken as the basis of the inter-nucleon potential described by Yukawa:

$$\frac{1}{c^2}\frac{\partial^2 \psi}{\partial t^2} = \nabla^2\psi - \left(\frac{m_\pi c}{\hbar}\right)^2\psi = \nabla^2\psi - \left(\frac{1}{r_\pi}\right)^2\psi \quad , \tag{2.1}$$

where ($r_\pi = \hbar/m_\pi c = 1.462$ fm) is the pion Compton radius. If we assume that this wave amplitude Ψ is proportional to potential, then for a static potential the time dependent term is dropped, and in a spherically symmetric form the required solution of (2.1) is Yukawa's potential:

$$V(r) = -a_\chi \frac{\exp-(r/r_\pi)}{r} \quad , \tag{2.2}$$

where a_χ represents an effective hadronic/nuclear charge.

Although this attractive potential appears to fit the data for nucleon-nucleon ranges beyond 1.5fm, the measured force becomes repulsive like a hard core potential below 0.5fm. Overall, the "Paris potential" derived by Lacombe et al (1980) is commonly accepted as providing the best fit to experiment. Meson exchange has been invoked for the attractive part, while the repulsive core is phenomenological. Comparisons of the Paris and other potentials have been illustrated by Signell (1980) and Bugg (1981).

We shall now derive a more accurate relativistic expression for the field of a quiescent nucleon (neglecting spin), as would be measured by a theoretical infinitesimal test particle. This will not be exactly the same as would be experienced by an equally massive nucleon in a collision because of kinetic energy involvement. Furthermore, this mesonic field is permanent, and independent of the strong interaction mediated by gluons between the constituent quarks in the nucleon.

3.   Application of Einstein's equations

In order to use Einstein's equations to interpret the hadronic force in a way compatible with the long-range electromagnetic and gravitational forces, the potential energy function might be expected to have the simple form:

$$\gamma = \left\{ 1 + \frac{a_\chi V(r)}{m_p c^2} \right\} \quad . \tag{3.1}$$

Here m_p is the proton mass and $V(r)$ is given by (2.2), and we define γ^2 as the metric tensor component, (see Paper 1, Section 1.8, and Wayte 1983). However, this form leads to regions of *negative* meson-field energy. A physically acceptable form, compatible with Poisson's Equation for a mesonic field around a proton is:

$$\gamma = \left\{ 1 - 2 \left(\frac{a_\chi^2}{m_p c^2} \right) \frac{\exp - (r / r_\pi)}{r} \right\}^{1/2} \quad , \tag{3.2}$$

which approximates to (3.1) for a weak field. Given that we need $(\gamma = 0)$ at the *effective* proton radius $(r_p = \hbar/m_p c = 0.2103\text{fm})$, then upon substituting $(r = r_p)$ we get:

$$2 \left(\frac{a_\chi^2}{m_p c^2} \right) \exp - \left(r_p / r_\pi \right) = r_p \quad , \tag{3.3}$$

therefore,

$$\gamma = \left\{ 1 - \left(\frac{r_p}{r} \right) \exp - \left(\frac{r - r_p}{r_\pi} \right) \right\}^{1/2} . \tag{3.4}$$

Now, the *general* coordinate potential V_c should probably be related to the metric tensor component through an expression like (3.1):

$$\gamma = (1 + a_\chi V_C / m_p c^2) \quad , \tag{3.5}$$

therefore, (3.4) yields:

$$a_\chi V_c = \left(m_p c^2 \right)(\gamma - 1) = \left(m_p c^2 \right) \left[\left\{ 1 - \left(\frac{r_p}{r} \right) \exp - \left(\frac{r - r_p}{r_\pi} \right) \right\}^{1/2} - 1 \right]. \tag{3.6}$$

This V_c is the empirical potential and it approaches double the depth of Yukawa's potential (2.2) as r decreases to r_p . The nucleon hadronic charge a_χ may be calculated from the *weak-field* approximation of (3.6), and letting $V_c \approx V(r)$ from (2.2):

$$\frac{a_\chi V_c}{m_p c^2} \approx -\left[\left(\frac{r_p}{2}\right)\exp\left(\frac{r_p}{r_\pi}\right)\right]\left(\frac{1}{r}\right)\exp-\left(\frac{r}{r_\pi}\right) \approx \frac{a_\chi V(r)}{m_p c^2} \quad . \tag{3.7}$$

Then by introducing $[r_p = 137(e^2/m_p c^2) = 0.2103 \text{ fm}]$ and $(r_\pi = 1.462 \text{ fm})$; where e is the electronic charge, we have:

$$a_\chi^2 \approx \left(\frac{m_p c^2 r_p}{2}\right)\exp\left(\frac{r_p}{r_\pi}\right) \approx 79e^2 \quad . \tag{3.8}$$

The hadronic interaction for nucleons is therefore 79 times stronger than the electromagnetic interaction; and the nucleonic coupling constant χ_N is definable as:

$$\chi_N = \frac{a_\chi^2}{\hbar c} \approx 79\left(\frac{1}{137}\right) \approx \frac{1}{\sqrt{3}} \quad . \tag{3.9}$$

Result (3.8) also follows from the strong-field condition of (3.3), so potential (3.6) is fully acceptable.

As derived for the electromagnetic and gravitational forces, the energy-momentum tensor components for a conserved spherically-symmetric radial field are:

$$8\pi\left(\frac{\chi}{c^4}\right)T_1^1 = 8\pi\left(\frac{\chi}{c^4}\right)T_4^4 = \frac{1}{r^2}\frac{d}{dr}\left[r(1-\gamma^2)\right] \quad , \tag{3.10}$$

$$8\pi\left(\frac{\chi}{c^4}\right)T_2^2 = 8\pi\left(\frac{\chi}{c^4}\right)T_3^3 = \frac{-1}{2r^2}\frac{d}{dr}\left[r^2\frac{d}{dr}(\gamma^2)\right] \quad , \tag{3.11}$$

(see Paper I, and Wayte 1983); χ is the NN hadronic constant, which evaluates to $(137e^2/m_p^2)$. This expression for momentum/stress density T_2^2 is the relativistic form of Poisson's Equation, so from substituting (3.2) in (3.11) we have:

$$8\pi\left(\frac{\chi}{c^4}\right)T_2^2 = \frac{(a_\chi^2/m_p c^2)}{r_\pi^2}\left(\frac{1}{r}\right)\exp-\left(\frac{r}{r_\pi}\right) \quad . \tag{3.12}$$

Similarly, the energy density T_4^4 is given by:

$$8\pi\left(\frac{\chi}{c^4}\right)T_4^4 = \frac{(a_\chi^2/m_p c^2)}{r_\pi}\left(\frac{-2}{r^2}\right)\exp-\left(\frac{r}{r_\pi}\right) \quad . \tag{3.13}$$

Integration of T_4^4 over all elemental shells from r_p to infinity yields the total mesonic field energy (W) as follows:

$$2\left(\frac{\chi}{c^4}\right)\int_{r_p}^{\infty} T_4^4 4\pi r^2 dr = \left[2\left(\frac{a_\chi^2}{m_p c^2}\right)exp-\left(\frac{r}{r_\pi}\right)\right]_{r_p}^{\infty} = -r_p = -\left(\frac{\chi m_p}{c^2}\right) \quad, \quad (3.14)$$

then,

$$W = \int_{r_p}^{\infty} T_4^4 4\pi r^2 dr = -(\tfrac{1}{2})m_p c^2 \quad . \tag{3.15}$$

Here, the negative sign indicates an attractive field constituting exactly one half of the proton mass. Analogous to the electron, half the proton mass resides in a core which supports the field. This proton core material is actually located in a torus, rotating at velocity c at mean radius r_p ; which gives the proton its spin [$\tfrac{1}{2}\hbar = (m_p /2)cr_p$]. The mesonic field propagates radially out and back and does not rotate.

Regarding this field, it is believed that each field-meson actually has equivalent mass m_π' which is a small fraction ($1/137^2$ say) of a free-pion mass m_π . A smooth copious field of 'bia-mesons' is thereby produced rather than a disjointed field of only 3 or 4 mesons. All the previous analysis remains valid if a reduced Planck constant (h′ << h) is assumed to go with the 'bia-meson' mass such that the field range is unchanged, ($r_\pi = \hbar$′ /m_π′c).

From (3.10), (3.12) and (3.13) the lateral stress T_2^2 relative to radial stress T_1^1 in the field is given by:

$$T_2^2 / T_1^1 = -r/2r_\pi \quad . \tag{3.16}$$

This is very different from the electromagnetic field in which the quanta have unitary helicity. It indicates that the field bia-mesons propagate radially at the velocity of light (since $T_1^1 = T_4^4$) but spin at a lower velocity when $r < 2r_\pi$. At larger radii, velocities greater than c are theoretically permissible for mechanisms within particles. A bia-meson therefore takes the form of a vortex, which decreases exponentially in energy from base to apex.

Total lateral stress may be found by integrating T_2^2 over all space beyond r_p :

$$\int_{r_p}^{\infty} T_2^2 4\pi r^2 dr = \left(1 + \frac{r_p}{r_\pi}\right)\frac{m_p c^2}{2} \quad . \tag{3.17}$$

Finally, the solution of (2.1) is the wave amplitude ψ, which must take the same form as Yukawa's potential in (2.2); therefore according to (3.12), ψ is proportional to the lateral stress/momentum density. This wave amplitude is not proportional to the real potential V_C, but is related through:

$$\left(1 + k\psi\right) = \left(1 + \frac{a_\chi V_C}{m_p c^2}\right)^2 \quad,$$ (3.18)

where k is a constant.

4.   Hard core repulsion

Hard core repulsion exists between like nucleons but not between a nucleon and an anti-nucleon; see Klempt et al. (2002). This agrees with the electromagnetic force in which electrons repel each other but attract positrons. Since the difference between electrons and positrons is helicity only, it will be postulated that hard-core repulsion is to do with helicity. There is then no need for a separate, repulsive quantum field which would modify energy distribution in the above bia-meson field and change (3.15). However, regular bia-mesons from nucleons are identical and simply expected to produce an attractive field for all radii according to (3.10)-(3.13). Consequently, actual repulsion between nucleons will be attributed to some form of helical field modulation which converts normal attraction into very strong short-range repulsion. Such modulation could be produced by the spinning proton core torus which supports the field. That spin frequency is (m_p / m_π) times greater than the meson Compton frequency, therefore the repulsion could be that much greater. Propagation of the modulation into the field is expected to be compatible with (2.1) and (2.2), wherein m_π would be changed to m_p ; so the proposed *overall* potential exhibits a reversal of the attractive potential in the short-range only. We must incorporate this effect into the metric tensor component by modifying (3.4) to:

$$\gamma_{hc} = \left\{1 - \left(\frac{r_p}{r}\right)\left[1 - \left(\frac{m_p}{m_\pi}\right)\left(\frac{r_p}{r}\right)\exp-\left(\frac{r - r_p}{r_p}\right)\right]\exp-\left(\frac{r - r_p}{r_\pi}\right)\right\}^{1/2} .$$ (4.1)

This describes a *modification* of the existing bia-meson field, rather than simply adding a repulsive field to it. At very short range ($r \approx r_p$), this approximates to a satisfactory form:

$$\gamma_{hc} \approx \left\{ 1 - \left(\frac{r_p}{r} \right) + \left(\frac{r_p r_\pi}{r^2} \right) \exp - \left(\frac{r - r_p}{r_p} \right) \right\}^{1/2} \rightarrow \{7\}^{1/2} \ . \tag{4.2}$$

So, (4.1) is viable and the empirical overall nucleon potential is given by:

$$a_\chi V_{hc} = \left(m_p c^2 \right) \left(\gamma_{hc} - 1 \right) \ . \tag{4.3}$$

This is plotted in Figure 1, and at larger radii it appears stronger than the Paris tensor component illustrated in Figure 2 for comparison.

It is possible that the proposed field modulation also affects the attraction between a nucleon and anti-nucleon. By changing (m_p) to $(-m_p)$ in (4.1), the attraction potential is increased noticeably beyond (3.6) at smaller radii, as shown by the dotted line in Figure 1.
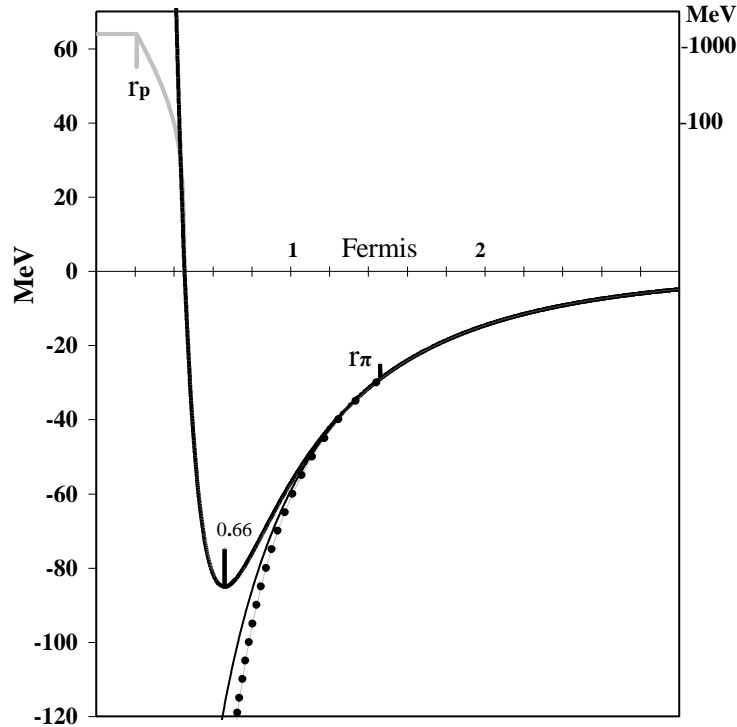

Figure 1. The nucleon-nucleon potential. **Thin line** shows the attractive component according to equation (3.6). **Bold-line** shows the total potential with hard-core repulsion, according to equation (4.3). **Grey-line top-left** is to include radii down to r_p , corresponding with the logarithmic scale on the right. **Dotted-line** shows the *enhanced attraction* between a nucleon and an anti-nucleon, caused by the field modulation.
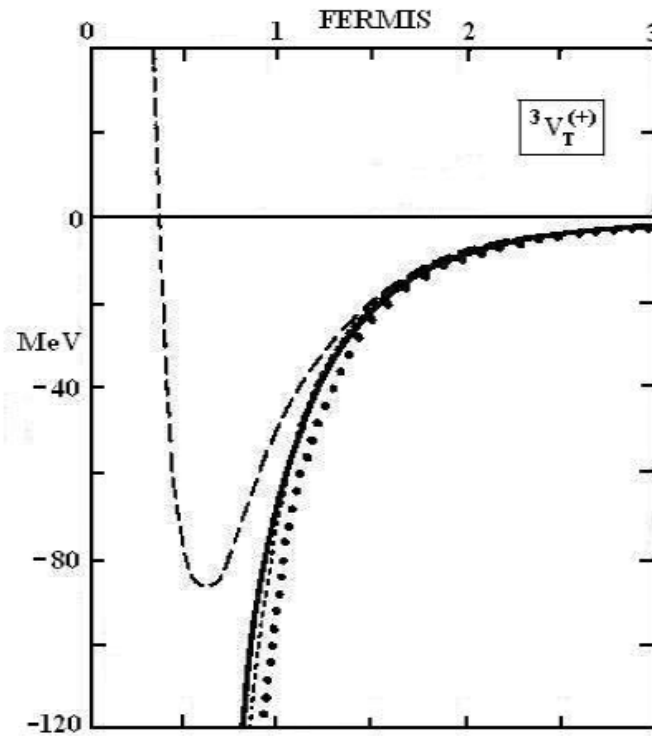
Figure 2.   The Paris tensor potential (- - -) and other potentials, copied from Signell (1980) for comparison with Figure 1.

Although a spherically symmetric bia-meson field has been assumed so far, the proton actually produces a toroidal field which approximates to a spherical field at large radius ($r \gg r_p$). This will undoubtedly affect high energy NN collision results, especially with regard to spin polarisation.

As mentioned earlier, this native field (4.3) is only experienced by small test particles because massive nucleons in collision cause modifications to the field source. For example, in a head-on collision of two nucleons, the incident kinetic energy is steadily absorbed and converted to mass energy until the particles come to rest momentarily. This increase in mass from m_p to m_p' causes the nucleon to shrink in size to $r_p' = \hbar/m_p'c$. At the same time, potential V_{hc} in (4.3) will increase. So both the nucleons become smaller and harder, unless disintegration occurs. If for example, both the nucleons were to have the same initial kinetic energy, (KE = $m_p c^2$ say) then the abscissa in Figure 1 would become

half and the ordinate would become double at the instant of closest approach in a head-on impact.

5.   Proton magnetic moment

Previous papers on the electron and muon showed how the magnetic moment analysis could involve all the component parts of those particles, from spin-loop through to fundamental elements. Likewise here, the measured proton magnetic moment exhibits features which can be directly attributed to substructure components, in common with the electron. Electromagnetic strength factors, 137, 37.7, 24 and 50 are identified in the component parts, in terms of simple geometry.

In this model, a proton is to consist of 9 pieces of approximate muonic mass arranged in two ranks of 3 parts (see Figure 3), bound by gluons and electromagnetic guidewaves. The larger rank is the spin-loop of spin $\frac{1}{2}\hbar$, and is equivalent to the 3 quarks of QCD theory; but since they are very different from quarks they will be called trineons. These parts have equal mass and travel around a Lagrange system (see Montgomery, 2001), which is known to be a system of minimum action. Probably, the 3 parts in a rank differ in phase by $2\pi/3$, and this could be responsible for the so-called quark colour phenomenon. A trineon is complex, consisting of 3 complex pearls, each part consisting of 37 grains, which consist of 137 mites, which contain 50 elements each. We shall see in Section 7 that the proton creation is most easily understood if it happens via seed growth, starting with the spin-loop and working downwards to smaller elements, which can only be created in situ as space becomes available. As for the electron, the grains, mites, and elements are treated like particles, but they are actually the individual turns of a helix around the periphery of the next larger particle.

Given that the proton spin is $\frac{1}{2}\hbar$, then the expected magnetic moment of the spin-loop would be one nuclear magneton:

$$\mu_s = \text{current} \times \text{area} = \left(\frac{e}{2\pi r_p / c}\right)\left(\pi r_p{}^2\right) = \frac{e\hbar}{2m_p} = \mu_N \ . \tag{5.1}$$

The measured value is almost 3 times this:

$$\mu_p = \mu_N \text{ x } 2.792\ 847\ 356\ (23). \tag{5.2}$$

Our proton model will produce a concise expression for μ_p as:

$$\mu_p / \mu_s = 2.792\,847\,357$$

$$= 3\left\{1 + [(2\pi\alpha^{-1}) + 1]^{-1}\left\{1 - 3\left(\pi^3\alpha / 4e_n\right)\left[1 + (3\varepsilon)\left\{1 - (\delta/2)\left[1 - (\pi\alpha/2)\left\{1 + (\mu\pi/e_n)\right\}\right]\right\}\right]\right\}\right\}. \quad (5.3)$$

Here the fine structure constant has been taken as the empirical value:

$$\alpha^{-1} = 137.035999679(94) \approx 137, \quad\quad (5.4a)$$

while the other constants have the same values as for the electron, but they have different roles:

$$\delta^{-1} = 12\pi \sim 37.7, \qquad \varepsilon^{-1} = 24, \qquad \mu^{-1} = 16\pi \approx 50, \quad\quad (5.4b)$$

and $e_n = 2.718281828$ is the natural logarithm base.

Analysis of the magnetic moment equation (5.3) will involve some properties already seen in electron and muon structures, plus some new features. The first factor 3 implies that each trineon behaves as if it has unit charge e^+ when interacting with an applied external magnetic field, even though the exterior charge of the proton is e^+. Subsequent terms cover magnetic moments of 3 pearls per trineon, with their constituent grains, mites and elements, which are all physically much smaller particles.

The first curly bracket of (5.3) is identical to that in the electron model, and serves to include the self-interaction electromagnetic energy around the proton spin-loop, which increases the effective circulating charge. This energy is nominally $(e^2/2\pi r_p)$ but it has to be supplied by the proton itself, so it is reduced slightly to:

$$\Delta E = \left(\frac{e^2}{2\pi r_p}\right)\left[\frac{(m_p c^2 - \Delta E)}{m_p c^2}\right], \quad\quad (5.5a)$$

which gives the required normalized value:

$$\Delta E / m_p c^2 = [(2\pi\alpha^{-1}) + 1]^{-1}. \quad\quad (5.5b)$$

Each part of the second curly bracket in (5.3) may be explained by expanding each term:

$$1 - \left(\frac{(3)137(\pi/e_n)}{[137(2/\pi)]^2}\right)\left[1 + \left(\frac{(3)24}{24^2}\right)\left\{1 - \left(\frac{37.7}{2\times 37.7^2}\right)\left[1 - \left(\frac{(2/\pi)137}{[137(2/\pi)]^2}\right)\left\{1 + \frac{(2/\pi)(\pi/2)(\pi/e_n)50}{50^2}\right\}\right]\right\}\right].$$

$$\text{3 trineons} \qquad \text{3 pearls} \quad \text{37 grains} \qquad \text{137 mites} \qquad \text{50 elements} \qquad (5.6)$$

For clarity, the approximate forms of α, δ, ε, μ have been used, and the particles being described are noted underneath. In the following explanation of each term, the 'current x area' definition (5.1) is consistently applied with regard to current flow and particle areas.

The first round bracket in (5.6) represents the contribution to the magnetic moment from 3 trineons, running as cycloids, anti-parallel to the spin-loop, see Figure 3. A trineon is $137(2/\pi)$ times smaller than the spin-loop, so the denominator expresses the corresponding relative area. It spins with enhanced velocity $c' = c(\pi/2)$. The numerator factor 137 represents current flow around the 137 gluonic loops which constitute a trineon itself, (formed into 3 clumps/pearls). Factor (π/e_n) is weighting for these gluons.
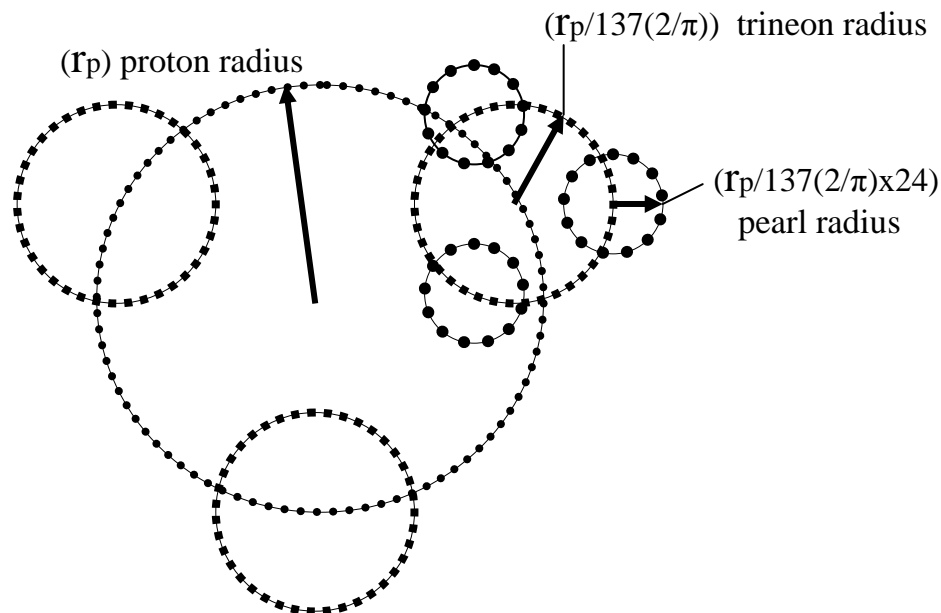

Figure 3.   Schematic diagram of a proton which consists of 2 ranks incorporating 3 trineons and 3 pearls. A pearl has approximately the mass of a muon.

The second round bracket represents the contribution from the 3 pearls, running as cycloids, around and parallel to their trineons, see Figure 3. A pearl is 24 times smaller than a trineon so the denominator expresses relative area. It spins with velocity c'. The numerator factor 24 is interpreted as current flow around the 24 gluonic loops which constitute the pearl itself, (braided into a peripheral helix of grains).

The third round bracket represents contribution from the 37 grains running helically, (probably left-handed), around each pearl circumference. A grain spins at velocity c', and is 37.7 times smaller than a pearl so the denominator expresses relative area. Attenuation factor (1/2) may be due to the helical propagation around the cycloidal pearl.

The fourth round bracket represents the contribution from current flow around 137 mites running helically around each grain circumference. A mite spins at velocity c', and is $137(2/\pi)$ times smaller than a grain, so the denominator expresses relative area. The attenuation coefficient $(2/\pi)$ applies to mites and their constituent elements because of their changes in orientation as they run around a grain. Mite areas, projected parallel to the spin-loop, are thus reduced by the factor $(2/\pi)$ on average.

Finally, the last bracket represents the contribution from 50 elements running helically around each mite circumference. An element spins at velocity c, and is 50 times smaller than a mite so the denominator expresses relative area. The additional attenuation coefficient $(2/\pi)$ applies to elements because of their changes in orientation as they move. Their areas, projected parallel to the spin-loop in *two* axes, are reduced to $(2/\pi)^2$ on average. The weighting factor $(\pi/2)$ is attributed to the element spin velocity being c while its propagation velocity is c' around its mite circumference; as seen for the grain/mite transition in the electron model. Coefficient (π/e_n) accounts for the field energy associated with the elemental material.

The 50 elements per mite are the actual source of proton electromagnetic field quanta, and probably have right-handed helicity like positrons. However, in experiments on electron and neutrino scattering from protons, the pearls behave as if they have left-handed helicity. Consequently, if the elements should also have left-handed helicity, then the field quanta must peel-off or bifurcate from their elements, with opposite hand.

6.   Proton mass

Analysis of the muon (Paper 2) showed how its mass is related to the electron mass in terms of binding energy loss and magnetic coupling effects. If proton mass is physically related to muon mass, it can also reveal a binding energy term:

$$m_p = 8.880243389 \times m_\mu \approx 3 \times \left[3\left(1 - \frac{1}{2 \times 37.7}\right) m_\mu \right] \quad , \tag{6.1}$$

where ($m_p = 1836.15267247(80) \; m_e$) and ($m_\mu = 206.768 \; 2823 \; (52) \; m_e$).

At first sight, this expression could imply that a proton is just a collection of 9 muons; but in fact, the structure within a proton pearl is very different from the structure of a *free* muon. The bracket on the right could be taken to describe binding energy of 3 pearls in a *trineon*, as if the pearls remain by attraction around the trineon circumference with a binding energy of ($m_\mu c^2/2 \times 37.7$) per pearl.

We shall see in Section 7 that the proton core is found to consist of a single filament of matter, winding through every element in every part, in series. Then from Section 5, the proton elemental mass is given by:

$$m_{el/p} = m_p / [(3 \times 137)(3 \times 24)(37.7)(137)(50)] \quad . \tag{6.2}$$

For comparison, the electron structure analysis in Paper 1 showed how the electron elemental mass was given by:

$$m_{el/e} = m_e / [(137)(137)(37.7)(24)(50)] \quad . \tag{6.3}$$

The ratio of these different elemental masses is:

$$\frac{m_{el/p}}{m_{el/e}} \approx \frac{1836}{3 \times 3} \approx 204 \approx \frac{m_\mu}{m_e} \quad . \tag{6.4}$$

7.   Creation of proton component parts

Just as the electron and muon were created in several separate stages by spiralling from previously created or newly generated seeds, so the proton structure is analysable from spin-loop to its most fundamental elements.   Using previous techniques and arguments from Paper 1, every step has to be compatible with other aspects of the model, and empirically sound.   The above magnetic moment analysis has been the essential basis of the following theory, with frequent reference to electron structure, given in Paper1.

7.1   Creation of a proton spin-loop

Proton design involves 3 trineons travelling cycloidally around the spin-loop at velocity c, aligned *antiparallel* to the spin-loop. For creation of the spin-loop from a small

seed, the proposed *spiralling plus seed-creation* equation is to be based on the following formula:

$$\{\ln(137/e_n) - \ln[1 + \ln(137/e_n)]\} + \{\ln 137\} \approx (2\pi^2/e_n) \ . \qquad (7.1.1)$$

Here the first two terms will cover spiralling open of the seed by a radial factor ($137/e_n \approx 50$), while the third term indicates that the seed itself will be created with 137 material loops on its circumference. After spiralling open from the seed radius ($r_{ps} \approx r_p/50$), this material separates into 3 trineons, (of 137 gluonic loops each). Given the spin-loop radius [$r_p = 137(e^2/m_p c^2) = 137 r_{po}$] and circumference ($'O_p = 2\pi r_p = z_p$), then (7.1.1) may be reduced to an action equation:

$$\left\{ \int_{'O_{ps}}^{'O_p} \frac{e^2}{z}\left[1 - \frac{v_z}{c}\right]\left[\frac{v_z}{c}\right] dt \right\} + \left\{ \int_{'O_{ps}/137}^{'O_{ps}} \frac{e^2}{z_h} \frac{dz_h}{c} \right\} \approx \left(\frac{\pi}{e_n}\right) \int_0^{2\pi} \left(m_p c r_{po}\right) d\theta \ . \qquad (7.1.2)$$

The spiralling term on the left describes how a proton circumference ($'O_p$) is formed by spiralling from the spin-loop-seed circumference ($'O_{ps} = 'O_p/(137/e_n)$). It confirms that a proton behaves as if it has charge e^+ throughout the process. In the second term, the circumference of the original seed ($'O_{ps}$) consists of 137 material loops wound in a helix of radius ($'O_{ps}/2\pi 137$), and created just before spiralling begins. These loops develop after the spiralling process into the 3 trineons. On the right, the action integral employs the original mass m_p in the spin-loop before any external pionic field has formed, (which would reduce m_p to $m_p/2$). The kinetic energy action is given using the classical proton radius ($r_{po} = e^2/m_p c^2$), analogous to the classical electron radius ($r_o = e^2/mc^2$) used in Paper 1. Weighting coefficient (π/e_n) accounts for internal field energy associated with the material energy.

7.2   Creation of a trineon.

Trineon design consists ultimately of a circumference of 3 complex pearls aligned *anti-parallel* to their trineon. A trineon has a radius r_o' which is $137(2/\pi)$ times smaller than the spin-loop r_p , and it rotates at a velocity $c' = c(\pi/2)$. The proposed spiralling plus seed-creation equation is to be based upon a formula somewhat like that for spin-loop creation:

$$\{\ln(24/e_n) - \ln(1 + \ln(24/e_n))\} + \{\ln 24\} \approx (\pi^3/e_n^2) \quad . \tag{7.2.1}$$

Given the classical proton radius expression ($r_{po} = e^2/m_p c^2$), then development of (7.2.1) in the usual way yields an action integral for each of the 137 loops produced above, prior to their condensing into 3 separate trineons:

$$\left\{\int_{'O_{0s}}^{'O_0} \frac{(e/137)^2}{z}\left[1 - \frac{v_z}{c'}\right]\left[\frac{v_z}{c'}\right]dt\right\} + \left\{\int_{'O_{0s/24}}^{'O_{0s}} \frac{(e/137)^2}{z_h}dt\right\} \approx \left(\frac{\pi}{e_n}\right)\int_0^{2\pi}\left(\frac{m_p c r_{po}}{137^2}\right)\frac{d\theta}{e_n} \quad . \tag{7.2.2}$$

The first term shows a trineon circumference ($'O_0 = z_p/137(2/\pi)$), being formed by spiralling from the trineon-seed circumference ($'O_{0s} = 'O_0/(24/e_n)$). In the second term, this original seed circumference has 24 material loops, in a helix of radius ($'O_{0s}/2\pi24$), created just before the spiralling begins.   These original 24 material loops grow and finally condense into 3 pearls (of 24 gluonic loops each) propagating around the trineon circumference at velocity c' while spinning at c' also. On the right side, the proton kinetic energy action is given, using classical r_{po} again. Weighting coefficient (π/e_n) accounts for field energy associated with the material energy. Factor ($1/e_n$) indicates that a second harmonic guidewave is in control.

7.3   Creation of a pearl.

A pearl periphery $'O_1$ consists ultimately of 37 grains which propagate helically around the circumference at velocity c' = c($\pi/2$), while spinning at c'. The pearl spiralling plus seed-creation equation is based upon a formula with some similarity to that for trineon creation:

$$\{\ln 37.7 - \ln(1 + \ln 37.7)\} + \{\ln 37.7\} \approx (\pi^3/2e_n) \quad . \tag{7.3.1}$$

Development of this in the usual way yields an action integral for each of the 24 loops produced above, prior to their condensing into 3 separate pearls:

$$\left\{\int_{'O_{1s}}^{'O_1} \frac{(e\alpha\varepsilon)^2}{\ell}\left[1 - \frac{v_\ell}{c'}\right]\left[\frac{v_\ell}{c'}\right]dt\right\} + \left\{\int_{'O_{1s/37.7}}^{'O_{1s}} \frac{(e\alpha\varepsilon)^2}{\ell_h}dt\right\} \approx \left(\frac{\pi}{e_n}\right)\int_0^{2\pi}\left(\frac{m_p c r_{po}}{2(137\times24)^2}\right)d\theta. \tag{7.3.2}$$

The first term covers spiralling growth of the pearl by factor 37.7 from a seed of circumference ($'O_{1s} = 'O_1/37.7$). Final pearl circumference is 24 times less than the trineon, ($'O_1 = 'O_0/24$) . In the second term, the original pearl-seed circumference ($'O_{1s}$)

has 37.7 material loops in a helix of radius ($'O_{1S}/2\pi37.7$), created just before spiralling begins. These 37.7 loops grow into the grainy helix, propagating around the pearl circumference at velocity c' while spinning at c'. On the right side, weighting coefficient (π/e_n) accounts for field energy associated with the material energy.

7.4   Creation of a grain.

A grain periphery $'O_2$ consists of 137 mites which travel around the grain at velocity c' while spinning at velocity c' also. The grain spiralling plus seed-creation equation is based on a formula like that for spin-loop creation:

$$\{\ln(137/e_n)-\ln(1+\ln(137/e_n))\}+\{\ln(137)\}\approx(2\pi^2/e_n)\ . \qquad (7.4.1)$$

This may be developed into an action integral:

$$\left\{\int_{'O_{2s}}^{'O_2}\frac{(e\alpha\epsilon\delta)^2}{\xi}\left[1-\frac{v_\xi}{c'}\right]\left[\frac{v_\xi}{c'}\right]dt\right\}+\left\{\int_{'O_{2s}/137}^{'O_{2s}}\frac{(e\alpha\epsilon\delta)^2}{\xi_h}dt\right\}\approx\int_0^{2\pi}\frac{m_p cr_{po}}{(137\times24\times37.7)^2}\left(\frac{2}{e_n}\right)d\theta\ . \ (7.4.2)$$

The first term covers spiralling growth of the grain by a factor ($137/e_n$) from a seed circumference [$'O_{2s}='O_2/(137/e_n)$]. Final grain circumference is 37.7 times less than the pearl, ($'O_2='O_1/37.7$). In the second term, the original grain-seed circumference ($'O_{2s}$) has 137 material loops, in a helix of radius ($'O_{2s}/2\pi137$), created just prior to spiralling. These grow in the grain final circumference into 137 mites (each of circumference, $'O_3='O_2/137(2/\pi)$) which propagate and spin at velocity c'. On the right-side, factor 2 is for weighting, and ($1/e_n$) indicates a second harmonic guidewave in operation here.

7.5   Creation of a mite.

A mite periphery contains ($16\pi\sim50$) elements, which travel around the circumference at velocity c' while spinning at c. The mite spiralling plus seed-creation equation is based upon a formula like that for grain creation:

$$\{\ln50-\ln(1+\ln50)\}+(\pi/2)\ln50\approx(2\pi^3/e_n^2)\ . \qquad (7.5.1)$$

Development of this in the usual way shows how a mite-seed evolves by spiralling open, according to this action integral:

$$\left\{\int_{'O_{3S}}^{'O_3}\frac{(e\alpha\epsilon\delta\alpha)^2}{\rho}\left[1-\frac{v_\rho}{c'}\right]\left[\frac{v_\rho}{c'}\right]dt\right\}+\left\{\int_{'O_{3S}/50}^{'O_{3S}}\frac{(e\alpha\epsilon\delta\alpha)^2}{\rho_h}dt\right\}\approx\left(\frac{\pi}{e_n}\right)\int_0^{2\pi}\frac{m_p c r_{po}}{(137\times24\times37.7\times137)^2}\left(\frac{2}{e_n}\right)d\theta$$

$$(7.5.2)$$

The first integral covers spiralling action for the mite increasing from a seed circumference $'O_{3s}$ to its final circumference ($'O_3 = 50\times'O_{3s}$), which is $137(2/\pi)$ times less than the grain, ($'O_3 = 'O_2/(137(2/\pi))$). The second integral represents scalar potential action of creating 50 elemental loops, which travel around the mite-seed circumference at velocity c' while spinning at c, prior to the mite spiralling process. On the right side, m_p is used rather than $m_p/2$ because this process applies prior to an external field forming. Weighting coefficient (π/e_n) accounts for field energy associated with the element material energy. Factor $(2/e_n)$ indicates a second harmonic guidewave is in operation here, with 2 times weighting.

A final mite circumference $'O_3$ then consists of a helix of 50 material elements travelling at c' around the circumference, while spinning at velocity c according to the formula:

$$\ln 50 \approx (\pi^2/e_n),\qquad\qquad(7.5.3)$$

which may represent an action integral:

$$\int_{'O_3/50}^{'O_3}\frac{(e\alpha\epsilon\delta\alpha)^2}{\rho_h}dt\approx\left(\frac{\pi}{e_n}\right)\int_0^{2\pi}\frac{m_p c r_{po}}{2(137\times24\times37.7\times137)^2}d\theta\quad.\qquad(7.5.4)$$

Weighting coefficient (π/e_n) appears in the magnetic moment analysis (5.6), and accounts for the field energy associated with the material energy. These 50 material elements in each mite are fundamental, and emit tethered electromagnetic field quanta with right-handed helicity.

8.   Gluons.

Experimentally, there is evidence that the 3 trineons in the proton spin-loop are bound together by charged gluons which emit colour force quanta. In Section (6) the proton mass analysis revealed some electromagnetic binding energy, as a small proportion of the overall mass. However, the gluon energy existing between trineons and pearls need not be explicitly stated. Each particle mass is inclusive of its gluon field energy, just as the

electron mass includes its field energy ($\frac{1}{2}m_ec^2$). When the proton is stressed in a collision, its strong gluon binding force operates to resist deformation and disintegration.

Our model of charmonium (pending) has employed the logarithmic potential developed by Quigg and Rosner (1979, pp217-223) to explain the gluon and colour field between a quark and anti-quark. For charmonium fundamental mass M_C and characteristic dimension r_q, the potential energy was found to be given by:

$$V(r) \approx \frac{M_C c^2}{2 \times 2^{1/2}} \ln\left(\frac{r}{r_q}\right) \quad , \tag{8.1}$$

For the proton here, this potential energy will be modified as follows:

$$V(r) = \frac{m_p c^2}{3 \times 2^{1/2}} \ln\left(\frac{r}{r_p}\right) \quad , \tag{8.2}$$

where we know ($r_p = 137(e^2/m_pc^2)$). Clearly, at equilibrium ($r = r_p$) the effective potential is zero, but the *field* must be operating continuously to confine the trineons against electromagnetic repulsion and centrifugal force. Then the metric tensor component for Einstein's equations will take the usual form:

$$\gamma = \left[1 + \frac{V(r)}{m_p c^2}\right] = \left[1 + \frac{1}{3 \times 2^{1/2}} \ln\left(\frac{r}{r_p}\right)\right] \quad . \tag{8.3}$$

Analogous to charmonium, the potential (8.2) will apply to a linear field, as in a tube of gluons linking the 3 trineons around the proton spin-loop. We propose that γ should be zero when the trineons [of radius $r_o' = r_p/(137(2/\pi))$], are almost touching in a circle of radius [$r_{ot} = r_p/69.6 = r_o'(1.25)$]; then (8.3) is satisfied.

We will let the proton binding field of gluons and colour quanta from the trineons be *confined* to a torus structure. The electron's spin-loop energy was calculated on the assumption of a *spherical field,* so let the trineon's *effective* area of emission be $4\pi r_o'^2$. We can then determine the total energy within a tube of effective cross-sectional area $4\pi r_o'^2$, by integrating the energy density.

There is a solution of Einstein's Equations, specifically for a conserved linear field, which will be proposed as equivalent to the toroidal field. For example, consider an ideally static field produced between a trineon placed at the origin and another trineon placed on the *x*-axis, say. The field of gluons is to be confined by a tube of cross-sectional

area $4\pi r_o'^2$ parallel to the axis. It will have components of the energy-momentum tensor as derived from Dingle's formulae (Tolman, 1934, p. 253), for the line element:

$$ds^2 = -\gamma^{-2}dx^2 - dy^2 - dz^2 + \gamma^2 dt^2 \quad . \tag{8.4}$$

These components are mathematically:

$$8\pi\left(\frac{Q}{c^4}\right)T_1^1 = 8\pi\left(\frac{Q}{c^4}\right)T_4^4 = 0 \tag{8.5a}$$

$$8\pi\left(\frac{Q}{c^4}\right)T_2^2 = 8\pi\left(\frac{Q}{c^4}\right)T_3^3 = -\frac{1}{2}\frac{d^2\gamma^2}{dx^2} = -\gamma\frac{d^2\gamma}{dx^2} - \left(\frac{d\gamma}{dx}\right)^2 \quad . \tag{8.5b}$$

Upon introducing γ from (8.3), with x set equivalent to r, we get the separate gluon and colour field tangential momentum densities:

$$8\pi\left(\frac{Q}{c^4}\right)T_2^2 = -\left(\frac{-\gamma}{3\times 2^{1/2}r^2}\right) - \left(\frac{1}{3\times 2^{1/2}r}\right)^2 \quad . \tag{8.6a}$$

T_2^2 is the effective momentum/stress density of the field of the source trineon, as seen at the position of the other trineon. Given the form of (8.6a), we shall infer that T_4^4 in (8.5a) cannot really represent zero energy density, and should be made physically compatible with T_2^2 by taking the form:

$$8\pi\left(\frac{Q}{c^4}\right)T_4^4 = -\left(\frac{-\gamma}{3\times 2^{1/2}r^2}\right) - \left(\frac{\gamma}{3\times 2^{1/2}r^2}\right) \quad . \tag{8.6b}$$

Analogous to (3.14), integration of this T_4^4 from ($r = r_{ot}$) to ($r = \infty$), will be taken to yield the separate and equal gluon and colour field energy components:

$$\left(\frac{Q}{c^4}\right)\int_{r_{ot}}^{\infty}T_4^4(4\pi r_o'^2)dr = -\left[\frac{-r_o'}{36\times 1.25}\right] - \left[\frac{r_o'}{36\times 1.25}\right] \quad . \tag{8.7}$$

The *modulus* of the first term on the right will be attributed to the energy of the gluons because the gluons from the 3 trineons travel in the same direction as other material around the spin-loop. Upon setting $[r_{ot} = Qm_p/c^2]$, analogous to the electron, then the maximum *gluon plus colour* field energy is $(1/9\pi)$ of the proton mass energy:

$$W = -\int_{r_{ot}}^{\infty}T_4^4(4\pi r_o'^2)dr = \frac{1}{9\pi}m_p c^2 \quad . \tag{8.8}$$

The tangential momentum density may be integrated to get a similar result:

$$\left(\frac{Q}{c^4}\right)\int_{r_{ot}}^{\infty} T_2^2\,(4\pi r_o'^2)\,dr = -\left[\frac{-r_o'}{36\times1.25}\right] - \left[\frac{r_o'}{36\times1.25}\right] \quad. \tag{8.9}$$

This means that the gluons plus colour field quanta have unitary helicity and propagate at the velocity of light.

Clearly, to interpret (8.5a) in real terms, it has been essential to introduce some prior knowledge of the real gluon and colour field into these solutions of Einstein's equations.

9. Electromagnetic charge uniqueness.

The electron and proton have charges which are accurately equal in magnitude, but their masses and internal mechanisms are very different. Furthermore, an electron-positron pair may be produced from high energy photons without reference to a proton. So it appears to be necessary for particle charges to be inherent and absolute.

Fermion spin is also absolute and may be related to charge. First, the theoretical classical radius of an electron, muon or proton has the form:

$$r_o = e^2 / m_o c^2 \quad. \tag{9.1}$$

This is based on the hypothesis that work would be done in assembling incremental charges against their mutual repulsion force, as may be expressed:

$$W = \iint_{q\,r} \frac{q\,dq}{r^2}\,dr = \left[\frac{1}{2}\frac{q^2}{r}\right]_{r=\infty,q=0}^{r_o,e} = \frac{1}{2}\left(\frac{e^2}{r_o}\right) \quad. \tag{9.2}$$

Then application of (9.1) gives $W = \tfrac{1}{2}m_o c^2$, as if the work done is stored in the particle as mass. The remaining $(\tfrac{1}{2}m_o c^2)$ must be attributed to the original charges or additional ballast. Even if such a classical compression process does not occur in reality, it is probable that particles are produced while conserving energy and charge, so that (9.2) and the inverse process of dispersion would be allowed.

Second, the theoretical radius (9.1) may not always exist physically, but the real spin radius is invariably given by $(r_s = 137 r_o)$. Thus for fermions, their spin is:

$$s = (m_o/2)c r_s = \hbar/2 \quad, \tag{9.3}$$

and the electric charge can be defined absolutely in terms of spin by:

$$e = \pm\{2cs/137\}^{1/2} \quad , \tag{9.4}$$

which is independent of particle mass, size, or detailed design. Then the large proton mass is effectively equivalent to work being done in forcing charge into the relatively small dimensions. Obviously, everything depends on particles having spatial volume with angular momentum, rather than being mathematical singularities.

Calculations of magnetic moment in Section (5) and creation-action in Section (7) depended upon the charge being divisible among the various substructures; so we need a charge formula applicable to the fundamental elements in a proton. For an *electron*, such a formula was found which was based upon allocating 3 curls of charge Δq to each *element*. In addition, there needed to be some field material holding the 3 charge-curls in place, effectively increasing their weight to $3(\pi/e_n)$. Now the total number of elements per electron was given in Paper 1 as:

$$n_e = 137 \times 137 \times 37.7 \times 24 \times 50 = 8.5405 \times 10^8 \quad . \tag{9.5}$$

and the electron total charge was therefore:

$$e = n_e \times 3(\pi/e_n) \times \Delta q = 2.9611 \times 10^9 \Delta q \quad . \tag{9.6}$$

When all the charge-curls were situated in a single circumferential helix of cross-sectional radius r_q and unitary pitch, the overall electromagnetic action was expressed as:

$$\int_x \frac{e^2}{x} dt \approx 3\left(\frac{\pi}{e_n}\right) \times \int_0^{2\pi} m_e cr_{oe} d\theta \quad , \tag{9.7}$$

where $(e^2/c = m_e cr_{oe})$ for the electron, and x varies from $2\pi r_q$ to $2\pi r_q\{n_e \times 3(\pi/e_n)\}$ with $(dt = dx/c)$. This primeval loop of around 3×10^9 charge-curls is a most basic definition of electron *charge*.

For a *proton* of unit charge e^+, the effective total number of elements will be taken as:

$$n_{tri} = 137 \times 24 \times 37.7 \times 137 \times 50 = 8.5405 \times 10^8 \quad . \tag{9.8}$$

The first term represents a spin-loop seed of 137 loops *before* separating into 3 trineons, as in creation equation (7.1.1). Each of these loops has a helix of 24 smaller loops according to (7.2.1), which later grow and separate into 3 pearls. Factor 37.7 represents the number of grains in each pre-pearl in equation (7.3.1). The next factor 137 is that for the mites in a grain, see (7.4.1). Finally, there are 50 elements per mite, as in (7.5.1). Clearly n_{tri} is equal

to n_e during the creation stages of the proton, which suggests that the final total charge should be the same as expressed in (9.6), even if it is distributed differently.

10.   Creation of a Neutron

The neutrons in a neutron star are formed, during the gravitational collapse of a massive star in a supernova event, because of great pressure forcing free electrons onto free protons. Consequently, a simple mechanical neutron model consists of a proton orbited by a heavy-electron, in such a way as to account for the neutron's magnetic moment and its empirical mass.

10.1   Magnetic moment

It was shown in Section (5) that the proton spin-loop has radius $[r_p = 137(e^2/m_p c^2)]$, and the measured magnetic moment is $[\mu_p \approx +2.792\ 847(e\hbar/2m_p)]$. Now, let there be a "heavy-electron" orbiting around a proton at selected radius $r_{he} = r_p(e_n\sqrt{3})$ with velocity c, which could produce a magnetic moment according to (5.1):

$$\mu_{he} = \left(\frac{-e}{2\pi r_{he}/c}\right)\left(\pi r_{he}^2\right) = -\frac{ecr_{he}}{2} = -\left(e_n\sqrt{3}\right)\times\mu_N \qquad . \qquad (10.1.1)$$

Then the resultant neutron magnetic moment should be around:

$$\mu_n \approx \mu_p + \mu_{he} \approx -1.915355\mu_N \ , \qquad (10.1.2)$$

which is close to the empirical value $\mu_n = -1.913\ 04273(45)\mu_N$.

10.2   Heavy-electron mass

Since the selected orbit radius r_{he} is less than the classical radius of a free electron $(r_o = e^2/m_e c^2)$, it is proposed that the compressed "heavy-electron" takes the physical form of the *core* of a *heavy-electron*. This core surrounds the proton as a thin torus of charged matter, as described in Paper 1. Work done to compress a free electron into this small core size in this location is effectively retained as the increased mass energy. Given r_{he} above, the heavy-electron mass might be as straightforward as:

$$m'_{he} = \left(\frac{e^2}{c^2 r_{he}}\right) = \alpha m_p\left(\frac{r_p}{r_{he}}\right) = 2.84589 m_e \ . \qquad (10.2.1)$$

However, the neutron mass $[m_n = 1838.683\ 6605(11)m_e]$ is only greater than the free proton mass by $2.5309\ 8803(11)m_e$; so we need to propose a better description of m_{he} . Namely, let the heavy-electron mass be given approximately by the formula:

$$m_{he}c^2 = 3m_ec^2\left\{1 - \frac{e^2}{3m_ec^2(2\pi r_{he})}\right\} = 2.547\,m_ec^2 \approx (m_nc^2 - m_pc^2) \ . \qquad (10.2.2)$$

Our interpretation of this is that the neutron's heavy-electron comprises 3 parts of nominal electronic mass, which are bound together by self-interaction of its electromagnetic guidewave force around the orbit $2\pi r_{he}$, (just as a trineon consists of 3 pearls bound by gluons). Existence of the 3 component parts will be supported by (10.2.7) and (10.3.4). This interpretation assumes that compression work has to be done to add energy $(1.5309m_ec^2)$ to a free electron mass, and the final electron is internally well bound and stable, unlike for (10.2.1). The proton does not affect this value of heavy-electron energy.

The original free electron spin-loop was compressed inwards by a factor of 137, to its seed size (r_{es} in Paper 1). This would happen in steps, rather than a single jump, because action needs to be quantised in a simple way. Possibly there would be 5 steps given by:

$$\ln 137 \approx \pi\left(1 + e^{-1} + e^{-2} + e^{-3} + e^{-4}\right) \qquad . \qquad (10.2.3)$$

For each step, the spin-loop material spirals-inward at azimuthal velocity c. Equation (10.2.3) may be developed into an action expression:

$$-\int_{2\pi r_e}^{2\pi r_{es}} \frac{e^2}{z}\,dt \approx \int_0^{2\pi} \frac{m_e}{2}\,cr_o\left(1 + \frac{1}{e_n} + \frac{1}{e_n^2} + \frac{1}{e_n^3} + \frac{1}{e_n^4}\right)d\theta \qquad . \qquad (10.2.4)$$

Here, the steps employ first to fifth harmonic guidewave frequencies, respectively. Clearly a single jump of size 137 would not accommodate velocity c, since $[\ln 137 \approx \pi(\pi/2)]$ implies velocity $[c' = c(\pi/2)]$.

The collapsing spiral has the simple form:

$$r = r_e \exp(-\phi/2\pi). \qquad (10.2.5)$$

If the azimuthal material velocity is constant at c, then $(rd\varphi = cdt)$ and consequently, the instantaneous electron circumference is

$$2\pi r = 2\pi r_e - ct \ . \qquad (10.2.6)$$

A controlling guidewave-loop collapses with the material, propagating at velocity c also. The total spiral rotates (4.92 ≈ ln137) times and has the same shape as for electron creation, even though the velocities are different. It is necessary that this compressed electron takes the *core* design (see Section 2 of Paper 1) because miniaturising the complete electron design does not produce the correct mass.

After the electron spin-loop has been compressed down to its core radius r_o, further pressure reduces it to r_{he}. This is quantisable, in terms of action, because $\ln(r_{he}/r_o) = \ln(2.84589) \approx \pi/3$, which leads to an action integral:

$$-\int_{2\pi r_o}^{2\pi r_{he}} \frac{e^2}{z} dt \approx \int_0^{2\pi/3} \frac{m_e}{2} c r_o d\theta \quad . \tag{10.2.7}$$

Phase factor $(2\pi/3)$ implies the separation of material into 3 particles during electron collapse, as allowed by (10.2.2).

Besides satisfying (10.2.2) for mass, the radius of the stable heavy-electron [$r_{he} = r_p(e_n\sqrt{3})$] is critical because quantisation is suggested by the formula:

$$\ln(r_{he}/r_p) \approx \pi/2 \tag{10.2.8}$$

The interpretation of this is that the toroidal heavy-electron transmits circular *feeler* guidewaves inwards from its position at r_{he} to the proton spin-loop at r_p. These are reflected back so continual interaction helps keep the electron in position. For an equivalent guidewave charge δe and mass δm, the action integral for this loop spiralling inwards and reflecting back is from (10.2.8):

$$-2\int_{2\pi r_{he}}^{2\pi r_p} \frac{(\delta e)^2}{z} dt \approx \int_0^{2\pi} \frac{\delta m}{2} c r_o d\theta \quad , \tag{10.2.9}$$

where $(\delta e/c = \delta m c r_o)$ and $(dz = cdt)$.

10.3 Neutron lifetime

Lifetime of the free neutron may be related to action around the heavy-electron in the same way as the muon lifetime was treated in Paper 2. The period of the heavy-electron is given by:

$$t_{he} = 2\pi r_{he}/c = 2.07526 \times 10^{-23} \text{ secs}, \tag{10.3.1}$$

while the measured neutron lifetime is:

$$\tau_n = 887.0 \text{ secs.} \tag{10.3.2}$$

Let $(c\tau_n)$ be equal to a number N_n of the heavy-electron circumferences (ct_{he}); then upon taking logarithms we get a familiar format:

$$\ln N_n = \ln(c\tau_n / ct_{he}) = 59.0172 \approx 137\left(\pi / e_n^2\right) \quad . \tag{10.3.3}$$

This may be developed, using $(e^2/c = m_{he}cr_{he})$, to give an expression for the action around N_n heavy-electron orbits:

$$\int_{2\pi r_{he}}^{N_n(2\pi r_{he})} \frac{e^2}{z} dt \approx 137 \times \int_0^{2\pi} \frac{m_{he}cr_{he}}{2}\left(\frac{1}{e_n^2}\right) d\theta \quad . \tag{10.3.4}$$

Here, $(1/e_n^2)$ on the right implies a third harmonic guidewave, which is perfect for stabilising the 3 components of the heavy-electron. Distance $c\tau_n$ could represent a coherence length for these guidewaves.

11.   Conclusion

A physical model of a proton has been developed which exhibits all known properties. Einstein's equations of general relativity have incorporated a Yukawa / Paris-type potential in order to define a hadronic force constant $\chi_N \approx \alpha(137/\sqrt{3})$. Proton mass has been related to muon mass, and the magnetic moment analysis has terms very similar to those employed for the electron. The 3 main constituents, named trineons, are nothing like quarks because they are very small and possess little spin themselves, but travel around the proton spin-loop together to generate observed proton spin $\frac{1}{2}\hbar$. Action integrals have been proposed for creating the entire substructure in separate stages, consecutively in chronological order from spin-loop through to fundamental elements. Gluon energy was quantified and found to be in agreement with other work on charmonium. The uniqueness of electronic charge has been explained in terms of a primeval loop of elementary charges, which satisfies a universal action integral. Finally, a neutron model was proposed, consisting of a proton orbited by a heavy-electron, which generates the empirical magnetic moment. Lifetime of a free neutron has been attributed to the finite coherence length of guidewaves operating around this heavy-electron.

Acknowledgement

I would like to thank Imperial College Library staff and R. Simpson for typing.

References

Bugg D V 1981 *Prog Part Nucl Phys.* **7** 47-112 ed DH Wilkinson, Oxford, Pergamon.

Fraunfelder H and Henley E M 1991 *Subatomic Physics, 2nd Ed*, Prentice-Hall Inc. NJ.

Iachello F 2004 *European Phys. J.* **A19** 29-34

Klempt E, et al. 2002 *Physics Reports* **368** 119-316

Krisch A D 1992 *Nuclear Phys.B Proc. Supp.* **25** 285-293

Lacombe M et al 1980 *Phys Rev* **C21** 861-873

Martin B R & Shaw G 1997 *Particle Physics, 2nd Ed*, J Wiley, England

Montgomery R 2001 *Not Amer Math Soc* **48** 471-475

Perkins D H 2000 *Introduction to High Energy Physics, 4th Ed*, Cambridge Univ. Press

Quigg C and Rosner J L 1979 *Phys. Reports* **56** 167-235

Sick I 2005 *Prog Particle Nuclear Phys* **55** 440-450

Signell P 1980 *Proc Telluride Conf on the (pn) Reaction and the Nucleon-Nucleon Force*
ed CD Goodman et al, NY, Plenum 1-21

Wayte R 1983 *Astrophys & Space Science* **91** 345-380

Wayte R (Paper 1) A Model of the Electron, submitted to *J Phys G*

Wayte R (Paper 2) A Model of the Muon, submitted to *J Phys G*